THERMOPHORESIS EFFECT OF DARCY-FORCHHEIMER POWELL EYRING FLUID WITH VARIABLE FLUID PROPERTIES

Dr M Sreedhar Babu[1*],

Abstract:
The current issue examines the effects of a non-uniform heat source, thermophoresis velocity, and activation energy on a Darcy-Forchheimer Powell Eyring towards a non-linear stretching sheet with changing thickness under the impact of variable thermal conductivity and spices diffusivity. Thermal conductivity and mass diffusivity in this issue are both intended to be linear functions of temperature and concentration. By using appropriate similarity variables, the flow system was turned into a system of PDEs for mathematical analysis, and subsequently into a system of ODEs. The Homotopy Analysis Method is used to arrive at the solution of the generated ODEs system. All important parameters' impacts are visually shown. A comparison with previous findings is done to corroborate the current findings. The temperature and concentration fields are enhanced while the velocity is depleted by the Forchheimer parameter. Temperature is increased by a non-uniform heat source and thermal conductivity characteristics. Thermophoretic velocity depletes the concentration while the spice diffusivity parameter increases it.

Key words:variable thickness, porous media, non-uniform heat source, Thermophoretic Velocity, activation energy.

[1*]Associate Professor, Dept. of Applied Mathematics,Yogi Vemana University, Kadapa, Andhra Pradesh,India-516005 Contact No:+91 9959656072 Email:msreedharyvu@gmail.com

***Corresponding author:-**Dr M Sreedhar Babu
[*]Associate Professor, Dept. of Applied Mathematics,Yogi Vemana University, Kadapa, Andhra Pradesh,India-516005 Contact No:+91 9959656072 Email:msreedharyvu@gmail.com

DOI: 10.53555/ecb/2024.13.01.25

1. Introduction

Regarding industrial and technological applications like the production of glass fibre, the processing of plastic sheets, aerodynamics, cooling and drying of paper, and lubricants, the study of heat and mass transfer is extremely important. There is currently no one formula that explains all the characteristics of non-Newtonian fluids. Different mathematical models are constructed in consideration of the character of the materials.Powell Eyring is a crucial model that is particularly useful in chemical engineering among those models. The Powell-Eyring model is unique among models since it is straightforward and stable.By taking into account the fluctuating thermal conductivity, Hayat et al. [1] closely examined the thermal properties of Powell-Eyring fluid. In a free parallel stream, Jalil et al. [2] succeeded in obtaining the self-similar solution of a Powell-Eyring fluid. The Powell Eyring fluid towards a stretched surface with a magnetic field was investigated statistically by Akbar et al. In order to examine the 3D MHD flow of Powell Eyring fluid, Hayat et al. [4] considered radiation. Powell Eyring fluid flow was reported by Rehman et al. [5] in a vertically positioned calendar. The MHD, nonlinear convective Powell Eyring fluid flow in the presence of Newtonian heating was clarified by Qayyum et al. [6]. By using a parabolic curve fitting strategy, Khan et al. [7] evaluated the physical properties of a Powell Eyring fluid containing chemically reactive spices.

Researchers have recently concentrated on the flow caused by a stretched sheet because of its substantial engineering applications. Examples include the manufacturing of rubber and plastic, paper, glass cooling, crystal growth processes, and polymer extrusion. In contrast to flat stretching sheet, however, stretching sheet with variable thickness has many more practical applications. The stretching sheet issue with variable thickness was first proposed by Fang et al. [8]. Incorporating slip conditions to the boundary layer flow caused by a stretched sheet of varying thickness, Khader and Megahed [9] obtained a numerical solution.By including heat production, Abdel-Wahedet al. [10] studied the MHD nano fluid generated by a stretched sheet of varying thickness. The characteristics of a Maxwell fluid on a sheet with varying thickness were investigated by Hayat et al. (11). The MHD Powell Eyring fluid produced by a nonlinear stretched sheet of changing thickness was examined by Hayat et al. [12]. In the presence or absence of mass transfer, Patil et al. [13] numerically investigated the double diffusion flow caused by a stretched sheet with varied thickness. By introducing a vanishing flux condition, Ghosh and Swati [14] studied mixed convective MHD nano fluid flow towards a stretched surface with changing thickness. According to Sharma et al. [15], melting and changing thickness have an impact on the MHD flow of a nano fluid across a metal sheet. A novel technique for the numerical solution of EMHD flow of nano fluid across a surface with variable thickness was developed by Irfan et al. [16]. The impact of mixed convection on a nanofluid flow towards a stretched sheet with changing thickness was investigated by Qasim et al. [17]. The effects of radiation and joule heating on the nano fluid flow towards a stretched sheet with changing thickness were carefully examined by Zahra et al. (18).

Many technical, industrial, and environmental systems use porous media to include convection. Only scant velocity and scant porosity are suitable for the use of the usual Darcy concept. When velocity is significant and when porosity is not uniform, the Darcy principle fails. By adding a component with a drag force constant increased by the square of velocity, the basic model is converted into a Darcy Forchheimer model. Examples include recovering organic molecules, understanding soil physics, changing living tissues, and storing waste, particularly gas waste.This setting has been worked on by several authors. In a Darcymedia, for instance, Aleem et al. [19] described the characteristics of chemical reaction and Newtonian heating of a nano fluid. In their discussion of the Darcy flow of a nano fluid, Hayat et al. [20] took internal and melting heat effects into account. The effects of homogenous-heterogenous chemical reactions in the Darcy flow of carbon nanotubes under convective conditions were the focus of studies by Alshomrani [21]. The Darcy-Forchheimer flow of a Casson fluid with magnetic influence was studied by Seth and Mandal [22]. The Darcy-Forchheimer MHD flow of a Casson fluid caused by a non-linear stretchable surface was described by Rasool et al. [23].

The effect of a heat source on temperature is an important phenomena in light of numerous physical applications. It can change the fluid's temperature profiles, which in turn affects how quickly particles are deposited in semiconductors, nuclear systems, and electrical devices. Depending on the environment and temperature, the type of heat source may be constant. Non-uniform heat source is integrated into this issue. This setting has been worked on by several authors. For instance, Reddy et al. [24] described the effects of slip circumstances and non-uniform source/sink on MHD nano fluid. Mehmood et al.'s [25] consideration of the non-uniform source/sink in the mixed convective MHD nano fluid. The effect of

non-uniform source/sink on the micro polar fluid was examined by Kumar et al. [26] by taking into account radiation and joule heating via porous medium. The effect of non-uniform source/sink on MHD Williamson fluid in a porous medium, as well as viscous dissipation, was discovered by Swain et al. [27]. The non-uniform source/sink was included in Kumar et al.'s [28] explanation of the heat transfer characteristics of an MHD Powell Eyring fluid over a wedge.

Thermophoresis is the process by which tiny molecules are transported from a warm region to a cool region. Tyndall [29] popularised the term "thermophoretic" in 1870.The effects of thermophoresis and joule heating on the radiative mixed convective flow of Jeffery fluid were explored by Shehzad et al. [30]. In their study [31], Kameswaran et al. examined the effects of thermophoretic on nonlinear convective flow caused by a vertical wall via a non-Darcy medium. In a non-Darcy medium, a vertical cone induces a mixed convective rotating flow that is described by Hariprasad et al.'s [32] numerical explanation. A nonlinear mixed convective flow over a vertical rotating cone immersed in porous media was the subject of discussion by Mallikarjuna et al. [33].

The smallest amount of energy required to start a chemical reaction is referred to as activation energy. Kinetic energy and potential energy are crucial for the bond-breaking process in chemical reactions.Molecules may lose kinetic energy as a result of incorrect collisions and be unable to finish the chemical process. In these circumstances, molecules require the least amount of energy to start a chemical reaction.Geothermal, hydrodynamic, and oil storage sectors all heavily rely on activation energy. On this context, several authors have worked. See [34-39], for instance.

Thermal conductivity and spice diffusivity were treated as constants in the investigations that were previously mentioned. However, in most cases, they may be used as variables. Thermal conductivity and mass diffusion were used as variables in Quereshi's (40) work on the Casson fluid. By taking into account temperature-dependent thermal conductivity and spice diffusivity, Nawaz et al. [41] studied the heat and mass transfer phenomena. In their paper on non-Newtonian fluids, Salahuddin et al. (42, 43) took variable diffusion and variable conductivity into account. By taking into account variable diffusion and variable conductivity, Waqas et al. [44, 45] reported on non-Newtonian fluids. The radiative flow of a Reiner-Philippoff fluid was described by Sajid et al. (46) in detail. In linear terms of temperature and concentration, they took into account thermal conductivity and spice diffusivity. Irfan et al. (47) examined the EMHD flow of a nano fluid by taking into account the linear relationship between temperature and concentration of the thermal conductivity and spice diffusivity.

2. Formulation

An incompressible, steady, 2D Darcy-Forchheimer Powell Eyring fluid towards a non-linear stretching sheet of variable thickness is explored. In this scrutiny, $y = A(x+c)^{\frac{1-n}{2}}$ gives the sheet thickness and $u_w = u_0\left(x+c\right)^n$ gives the sheet velocity where A is a constant whose value is very minimal, u_0 means reference velocity and c is dimensionless constant. In this scrutiny, non-uniform heat source along with thermophoresis velocity and activation energy are also included (see Fig. 1). Here, thermal conductivity (k) and the mass diffusivity (D) are supposed to be the linear functions of T and C .see ref [1].

$$k = k_\infty\left[1+\beta_1\theta\right] \quad (1)$$

$$D = D_\infty\left[1+\beta_2\phi\right] \quad (2)$$

In above Eqs. β_1, β_2 are so small parameters. If $\beta_1 = 0$ and $\beta_2 = 0$ then the problem becomes as the problem having constant thermal conductivity (k) and the mass diffusivity (D).

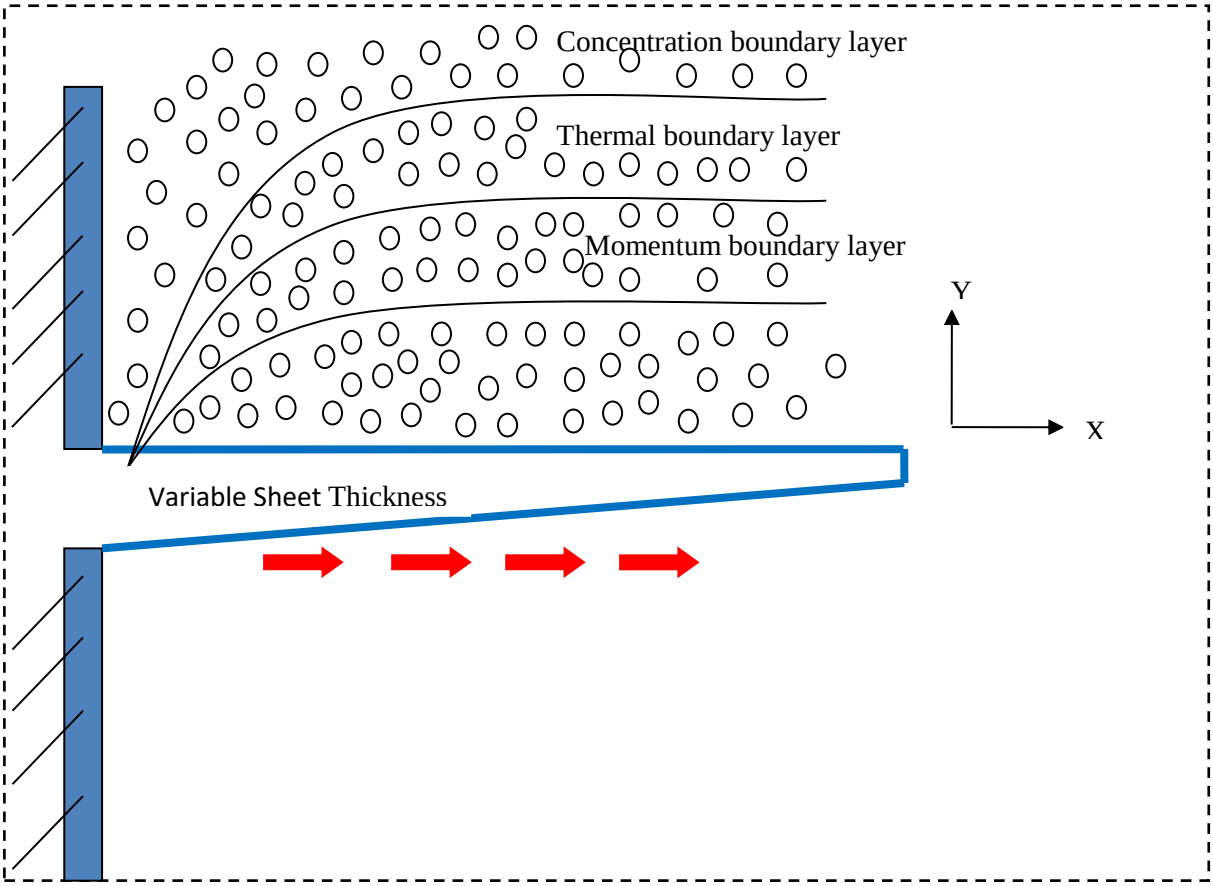

Fig. 1: Flow Diagram

The governing equations are:

$$\frac{\partial u}{\partial x}+\frac{\partial u}{\partial y}=0 \qquad (3)$$

$$u\frac{\partial u}{\partial x}+v\frac{\partial u}{\partial y}=\left(\vartheta+\frac{1}{\rho\beta d_1}\right)\frac{\partial^2 u}{\partial y^2}-\frac{1}{2\rho\beta d_1^3}\left(\frac{\partial u}{\partial y}\right)^2\frac{\partial^2 u}{\partial y^2}-\frac{\vartheta}{K}u-Fu^2 \qquad (4)$$

$$u\frac{\partial T}{\partial x}+v\frac{\partial T}{\partial y}=\frac{1}{\rho c_p}\frac{\partial}{\partial y}\left(k\frac{\partial T}{\partial y}\right)+\frac{k_\infty}{\rho c_p}\frac{u_w}{(x+b)\vartheta}\left[Q_1(T_w-T_\infty)g'(\eta)+Q_2(T-T_\infty)\right] \qquad (5)$$

$$u\frac{\partial C}{\partial x}+v\frac{\partial C}{\partial y}=D\frac{\partial^2 C}{\partial y^2}+\frac{\partial D}{\partial y}\frac{\partial C}{\partial y}-k_s^2\left(\frac{T}{T_\infty}\right)^s e^{-\frac{E_a}{k_1 T}}(C-C_\infty)-\frac{\partial}{\partial y}\left(V_T(C-C_\infty)\right) \qquad (6)$$

Boundary conditions:

$$\text{At } y=A(x+b)^{(1-n)/2}:$$
$$u=u_w,\ v=0,\ T=T_w,\ C=C_w$$
$$\text{At } y=\infty:$$
$$u\to 0,\ T\to T_\infty,\ C\to C_\infty. \qquad (7)$$

Here, u and v are velocity components in the direction of co-ordinate axis, ϑ signifies kinematic viscosity, ρ signifies density, $K=k_0(x+b)^{1-n}$ signifies variable permeability, $F=\dfrac{c_b}{(x+b)k_1^{\frac{1}{2}}}$ signifies non uniform coefficient of inertia, Q_1, Q_2 signifies the coefficients of space and temperature dependent heat source, $K_s^2=k_s^2(x+b)^{\frac{n-1}{2}}$

signifies coefficient of reaction rate and $V_T = \frac{\vartheta k_r}{T_r}\frac{\partial T}{\partial y}$ signifies Thermophoretic velocity.

After the implementation of subsequent transformation (8),

$$\eta = y\left[\frac{(n+1)u_0(x+b)^{n-1}}{2\vartheta}\right]^{\frac{1}{2}},$$

$$u = u_0(x+b)^n g'(\eta),\ v = \left(\frac{\vartheta u_0(n+1)(x+b)^{n-1}}{2}\right)^{\frac{1}{2}}\left[g(\eta)+\eta\frac{n-1}{n+1}g'(\eta)\right],$$

$$\theta = \frac{T-T_\infty}{T_w-T_\infty},\ \phi = \frac{C-C_\infty}{C_w-C_\infty} \qquad (8)$$

The governing Eqs. (5)-(7) with boundary conditions (9) are transformed as:

$$(1+\delta_1)g'''(\eta)-\frac{\delta_1\delta_2(n+1)}{2}g''^2 g''' + g(\eta)g''(\eta)-\frac{2n}{n+1}g'^2(\eta)-\frac{2}{n+1}k_p g'(\eta)-\frac{2F_r}{n+1}g'^2(\eta)=0 \qquad (9)$$

$$(1+\beta_1\Theta)\Theta''(\eta)+\beta_1\Theta'^2+\Pr g(\eta)\Theta'(\eta)+\frac{2}{n+1}\left[Q_1 g'+Q_2\Theta\right]=0 \qquad (10)$$

$$(1+\beta_2\,\Phi(\eta))\Phi''(\eta)+\beta_2\,\Phi'^2(\eta) + Sc\left(g(\eta)\Phi'(\eta)-\frac{2\sigma}{n+1}\left(1+\delta\Theta(\eta)\right)^s e^{-\frac{E}{1+\delta\Theta(\eta)}}-\tau\,\Theta'(\eta)\Phi'(\eta)-\tau\,\Phi(\eta)\Theta''(\eta)\right)=0 \qquad (11)$$

Boundary conditions:

$$\text{At}\ \eta=\alpha:\quad g'(\eta)=1\ g(\eta)=\alpha\frac{1-n}{1+n}\ \Theta(\eta)=1\ \Phi(\eta)=1$$

$$\text{For}\ \eta\to\infty:\quad g'(\eta)\to 0\ \Theta(\eta)\to 0\ \Phi(\eta)\to 0 \qquad (12)$$

To execute equations (9)-(11) mathematically, define

$$g(\eta)=f(\eta-\alpha)=f(\zeta),\ \Theta(\eta)=\theta(\eta-\alpha)=\theta(\zeta),\ \Phi(\eta)=\phi(\eta-\alpha)=\phi(\zeta) \qquad (13)$$

Now, equations from (7)-(10) can be transfigured as

$$(1+\delta_1)f'''(\varsigma)-\frac{\delta_1\delta_2(n+1)}{2}f''^2(\varsigma)f'''(\varsigma) + f(\varsigma)f''(\varsigma)-\frac{2n}{n+1}f'^2(\varsigma)-\frac{2}{n+1}k_p f'(\varsigma)-\frac{2F_r}{n+1}f'^2(\varsigma)=0 \qquad (14)$$

$$(1+\beta_1\theta(\varsigma))\theta''(\varsigma)+\beta_1\theta'^2(\varsigma)+\Pr f(\varsigma)\theta'(\varsigma)+\frac{2}{n+1}\left[Q_1 f'(\varsigma)+Q_2\theta(\varsigma)\right]=0 \qquad (15)$$

$$(1+\beta_2\,\phi(\varsigma))\phi''(\varsigma)+\beta_2\,\phi'^2(\varsigma) + Sc\left(f(\varsigma)\phi'(\varsigma)-\frac{2\sigma}{n+1}\left(1+\delta\theta(\varsigma)\right)^s e^{-\frac{E}{1+\delta\theta(\varsigma)}}-\tau\,\theta'(\varsigma)\phi'(\varsigma)-\tau\,\phi(\varsigma)\theta''(\varsigma)\right)=0 \qquad (16)$$

Boundary conditions:

$$\text{At}\,\varsigma = 0: \quad f'(\zeta) = 1,\ f(\zeta) = \alpha\frac{1-n}{1+n},\ \theta(\zeta) = 1,\ \phi(\zeta) = 1$$
$$\text{As}\,\zeta \to \infty: \quad f'(\zeta) \to 0,\ \theta(\zeta) \to 0,\ \phi(\zeta) \to 0. \qquad (17)$$

In above equations, α, k_p, F, Pr, Sc, σ, δ, E and τ signifies thickness parameter, Porous parameter, Forchheimer parameter, Prandtl number, Eckert number, Schmidt number, Reaction rate, parameter of Temperature difference parameter of activation energy and Thermophoretic parameter respectively whose values are given as

$$\delta_1 = \frac{1}{\mu\beta d_1}\ \delta_2 = \frac{u_o^2}{2\vartheta d_1^2 l^{1-3n}}\ \alpha = A\sqrt{\frac{u_0(n+1)}{2\vartheta}},\ k_p = \frac{\vartheta}{k_0 u_0},\ F_r = \frac{c_b}{k_1^{\frac{1}{2}}},$$
$$\Pr = \frac{\mu c_p}{k_\infty},\ Sc = \frac{\vartheta}{D_\infty},\ \sigma = \frac{k_s^2}{u_0},\ \delta = \frac{T_w - T_\infty}{T_\infty},\ E = \frac{E_a}{k_1 T_\infty},\ \tau = -\frac{k_r}{T_r}(T_w - T_\infty).$$

Skin friction coefficient

$$C_f = \frac{2\left(\mu + \frac{1}{\beta d_1}\frac{\partial u}{\partial y} - \frac{1}{6\beta d_1^3}\left(\frac{\partial u}{\partial y}\right)^3\right)_{y=A(x+c)^{\frac{1-n}{2}}}}{\rho u_w^2} \qquad (18)$$

On implementing (8) and (13)

$$C_f = \left(\frac{2(1+n)}{\mathrm{Re}_x}\right)^{\frac{1}{2}}\left[(1+\delta_1)f''(0) - \frac{n+1}{2}\frac{\delta_1\delta_2}{3}(f'''(0))^3\right]. \qquad (19)$$

Nusselt number

$$Nu_x = \frac{-(x+c)\left(\frac{\partial T}{\partial y}\right)_{y=A(x+c)^{1-n/2}}}{(T_w - T_\infty)}, \qquad (20)$$

On implementing (8) and (13)

$$Nu_x = -\left(\frac{(1+n)\mathrm{Re}_x}{2}\right)^{\frac{1}{2}}\theta'(0) \quad . \qquad (21)$$

Sherwood Number

$$Sh_x = \frac{-(x+c)\left(\frac{\partial C}{\partial y}\right)_{y=A(x+c)^{1-n/2}}}{(C_w - C_\infty)}, \qquad (22)$$

On implementing (8) and (13)

$$Sh_x = -\left(\frac{(1+n)\mathrm{Re}_x}{2}\right)^{\frac{1}{2}}\phi'(0) \ . \quad (23)$$

3. Solution methodology

By using the Homotopy Analysis Method, developed by Liao (48), the equations from (14) to (16) are numerically calculated.Here, the key reason for selecting the HAM approach is: (i) HAM solves nonlinear equations for both weak

and strong systems in a comparable way. (ii) The problem's restriction on large/small parameters does not apply to HAM. (iii) HAM creates a system to verify and enhance the convergence of the acquired solution. (iv) The enormous freedom to choose linear operators provided by HAM.
The method is initiated by appointing the starting guesses as:

$$f_o(\zeta) = 1 - e^{-\zeta} + \alpha \frac{1-n}{n+1},\ \theta_o(\zeta) = e^{-\zeta},\ \phi_o(\zeta) = e^{-\zeta} \quad (24)$$

Linear operators:

$$L_{f(\zeta)} = f'''(\zeta) - f(\zeta),\quad L_{\theta(\zeta)} = \theta''(\zeta) - \theta(\zeta),\ L_{\phi(\zeta)} = \phi''(\zeta) - \phi(\zeta) \quad (25)$$

Subject to

$$L_{f(\zeta)}\left(B_{11} + B_{22}e^{-\eta} + B_{33}e^{\eta}\right) = 0,\ L_{\theta(\zeta)}\left(B_{44}e^{-\eta} + B_{55}e^{\eta}\right) = 0,\ L_{\phi(\zeta)}\left(B_{66}e^{-\eta} + B_{77}e^{\eta}\right) = 0 \quad (26)$$

Where $B_{11}, B_{22}, B_{33}, B_{44}, B_{55}, B_{66}, B_{77}$ are arbitrary constants

Convergence of HAM:
The convergence and precision of HAM solution intensively depends on auxiliary parameters (h_f, h_θ, h_ϕ). To acquire the adequate values of (h_f, h_θ, h_ϕ), h-curves are framed which are depicted in figure 2, figure 3 and figure 4.it is perceived that the adequate values of h_f, h_θ, h_ϕ are [-1.4,-0.4], [-1.4,-0.7] and [-1.6,-0.6] respectively. Table 1 elucidates the convergence of proposed method. Table 1 gives the HAM solution at different approximations for $h_f = -0.9$, $h_\theta = -1.05, h_\phi = -1.1$

4. Results and discussions:
A nonlinear variable thickness stretched sheet with variable thermal conductivity and mass diffusivity is examined, as well as the effects of a non-uniform heat source, thermophoresis velocity, and activation energy on the flow of a Darcy-Forchheimer Powell Eyring fluid. The well-known HAM approach is used to numerically solve equations (14) through (16) by running the HAM. We demonstrated the HAM technique's correctness by making comparisons to the findings of Fang at el. [2] and Khader at el. [3]. Tables 2 and 3 show a nice correlation between HAM results and those of Fang at el. [2] and Khader at el. [3].

Effect of Porous parameter (k_p): Figures from 5 to 7reports on the effect of k_p. By amplifying k_p, a fall off sighted in fluid velocity where as an accretion is sighted in temperature and concentration fields. Growth in porosity develops a resistive force in the flow whichnarrows the momentum boundary layer. Hence, velocity depletes, temperature and concentration are amplified.

Effect of Forchheimer parameter (F_r): Figures from 8 to 10 narrates on the effect of F_r. Whenever F_r enhances, fluid velocity is decremented and the temperature and concentration profiles are raised. Increment in F_r dwindles the momentum boundary layer and fluid can't move smoothly. Eventually, velocity minimizes and temperature and concentration of the fluid maximizes.

Effect of Index parameter (n): Figures 11 to 13 imparts the effect of n.By amplifying the values of n, the velocity, temperature and concentration fields are also amplified. Here, $n = 1$ signifies flat sheet, $n < 1$ signifies growth in thickness and $n > 1$ signifies diminish in thickness. Here $n = 0$ Signifies linear flow and constant velocity. For $n < 1$ velocity depletes and increases for $n > 1$.

Effect of thickness parameter (α): Figure 14, Figure 15 and Figure 16 explains the effect of α. Increase in α causes a reduction in velocity, temperature and concentration fields. As sheet thickness increases, elongation of the sheet decelerates. As a consequence,velocity declines. Increase in α causes a transformation of little energy between the surface and fluid. Hence very less heat is transmittedbetween the surface and fluid. As a result diminish in temperature is detected. Similar behavior is detected for concentration fields.

Effect of Prandtl Number ($\Pr$): The result is shown in Figure 17. The thermal boundary layer thickens with increasing values, slowing the temperature. Prandtl Number and thermal

diffusivity are physically inversely connected. Stronger values display less thermal diffusivity due to the inverse relationship. Consequently, the temperature drops.

Effect of thermal conductivity parameter (β_1): Figure 18 reveals the effect of β_1. The rising values of β_1 causes a rise in temperature. Physically β_1 increases the collision between molecules which increases the heat energy transmission throughout the fluid. Hence temperature rises.

Effect of space and temperature dependent heat source: Figure 19 and figure 20 elucidate the effect of Q_1 and Q_2. When Q_1 and Q_2 are increased, temperature is also increases. Physically increasing values of Q_1 and Q_2 behaves like a heat generator whichobviously enhances the temperature.

Effect of Mass Diffusion Parameter (β_2): Figure 21 characterizes the effect of β_2 .As β_2 is raising; concentration boundary layer enhances and increment in the concentration of the fluid. Since mass diffusivity and fluid concentration are in proportion, enhanced values of β_2 amplifies the concentration significantly.

Effect of Schmidt Number (Sc): Figure 22 characterizes the effect of Sc . In general, Schmidt Number and mass diffusion are inversely related.This inverse relation causes depletion in concentration boundary layerfor stronger values of Sc and finally deceleration in concentration fields.

Effect of Thermophoretic Parameter (τ): Figure 23 characterizes the effect of τ . The amplified the values of τ causes a reduction in concentration fields. As τ is interconnected with temperature, it diminishes the concentration of spices in the entire flow region. Hence a reduction occurs in concentration.

Effect of Reaction Rate (σ): Figure 24 characterizes the effect of σ . Stronger values of σ declines the concentration boundary layer. As a consequenceconcentration reduces.

Effect of Temperature Difference Parameter (δ): Figure 25 unveils the Effect of δ . On amplifying the δ the extent of the concentration boundary layer becomes thin and concentration diminishes.

Effect of Activation Energy Parameter (E): Figure 26 characterizes the effect of E . Physically, E denotes the energy which is needed to stimulate the molecules in chemical reactions. It is recognized that larger values of E amplifies the extent of the concentration boundary layer. So, an upsurge occurs in fluidconcentration.

Table 3& table 4 represent the computed values of Skin friction, Nusselt Number and Sherwood Number. From table 3, a growth is detected in Skin friction for amplified values of n, α, k_p and F_r. A growth in Nusselt Number is detected for the amplified values of α and Pr .A reduction is detected in Nusselt Number for the amplified values of n, k_p, F_r, Q_1, Q_2 and β_1. From table 4, a growth is detected in Sherwood number for the amplified values of α, τ, σ *and* δ .A diminish is detected for amplified values of $n, k_p, F_r, \Pr, \beta_1, \beta_2, Sc$ *and* E.

5. Conclusions:

The current issue examines how a non-uniform heat source, thermophoresis velocity, and activation energy affect a Darcy-Forchheimer Powell Eyring towards a non-linearly stretched sheet with varying thickness under the impact of variable thermal conductivity and spices diffusivity.

- Velocity drops by amplifying k_p, F_r, α
- Velocity escalates by strengthening n.
- Temperature escalates by amplifying n, k_p, F_r, Q_1, Q_2 *and* β_1
- Temperature decelerates for strong values of α *and* $\Pr$.
- Concentration escalates for surging values of n, k_p, F_r, β_2 *and* E .
- Concentration decelerates for strong values of α, Sc, σ *and* δ .

Table 1: HAM solutions for $\delta_1 = 0.2,\ \delta_2 = 1.0,\ kp = 0.1,\ Fr = 0.3,\ \alpha = 0.3,\ n = 0.5,\ \Pr = 1.2,\ \beta_1 = 0.1,$ $Q_1 = 0.1, Q_2 = 0.01,\ \beta_2 = 0.1,\ Sc = 1.2,\ \tau = 0.2,\ \sigma = 0.5,\ \delta = 1,\ r = 0.5,\ E = 1,\ h_f = -0.9,$ $h_\theta = -1.05\, and\, h_\phi = -1.1.$

order	$-f''(0)$	$-\theta'(0)$	$-\phi'(0)$
1	1.06875	0.60100	1.24200
5	1.07018	0.58229	1.20829
10	1.07018	0.58326	1.20760
15	1.07018	0.58323	1.20759
20	1.07018	0.58323	1.20759
25	1.07018	0.58323	1.20759

Table 2: resemblance of $-\dfrac{d^2 f}{d\zeta^2}_{at\,\zeta=0}$ for dissimilar values of n

n	Fang et al. [2]	Khader et al. [3]	Present findings HAM	n	Fang et al. [2]	Khader et al. [3]	Present findings HAM
	$\alpha = 0.25$				$\alpha = 0.5$		
10	1.1433	1.1433	1.14332	10	1.0603	1.0603	1.06033
9	1.1404	1.1404	1.14039	9	1.0589	1.0588	1.05892
7	1.1323	1.1322	1.13229	7	1.0550	1.0551	1.05505
5	1.1186	1.1186	1.11859	5	1.0486	1.0486	1.04861
3	1.0905	1.0904	1.09049	3	1.0359	1.0358	1.03587
0.5	0.9338	0.9337	0.93382	2	1.0234	1.0234	1.02341
0	0.7843	0.7843	0.78428	0.5	0.9799	0.9798	0.97994
				0	0.9576	0.9577	0.95764

Table 3: variations in $-f''(0), -\theta'(0)$ as a function of $n, \alpha, k_p, F_r, \Pr, Q_1, Q_2, \beta_1$.

n	α	k_p	F_r	Pr	Q_1	Q_2	β_1	$-f''(0)$ HAM	$-\theta'(0)$ HAM
0	0.3	0.1	0.3	1.2	0.1	0.01	0.1	1.05126	0.69854
2								1.13504	0.47943
3								1.19067	0.45421
0.5	0.6							1.12079	0.66014
	0.8							1.15614	0.71304
	1							1.19282	0.76715
		0.3						1.19196	0.56813
		0.4						1.25000	0.56096
		0.5						1.30659	0.55403
			0.4					1.10951	0.57982
			0.5					1.14810	0.57652
			0.6					1.18603	0.57333
				0.7				1.07018	0.34877
				1.5				1.07018	0.70256
				2				1.07018	0.88626
					0.2			1.07018	0.49196
					0.3			1.07018	0.40036
					0.4			1.07018	0.30931
						0.02		1.07018	0.57229
						0.04		1.07018	0.54974
						0.06		1.07018	0.52622
							0.2	1.07018	0.54570
							0.3	1.07018	0.51339
							0.4	1.07018	0.48523

Table 4: variations in $-\phi'(0)$ as a function of $n, \alpha, k_p, F_r, \Pr, \beta_1, \beta_2, Sc, \varepsilon, \tau, \sigma, \delta, E$.

n	α	k_p	F_r	Pr	β_1	β_2	Sc	τ	σ	δ	E	$-\phi'(0)$
0	0.3	0.1	0.3	1.2	0.1	0.1	1.2	0.2	0.5	1	1	1.52214
2												1.16548
3												0.79690
0.5	0.6											1.27754
	0.8											1.32664
	1											1.37764
		0.3										1.19802
		0.4										1.19384
		0.5										1.18999
			0.4									1.20549
			0.5									1.20347
			0.6									1.20155
				0.7								1.22456
				1.5								1.20259
				2								1.19902
					0.2							1.20792
					0.3							1.20872
					0.4							1.20982
						0.2						1.13061
						0.4						1.00708
						0.6						0.91181
							1.3					1.27315
							1.7					1.51707
							2					1.67403
								0.5				1.34049
								1				1.57271
								1.5				1.81666
									0.6			1.28107
									0.7			1.35165
									0.8			1.41958
										1.2		1.30560
										1.4		1.40662
										1.6		1.51021
											1.1	1.19285
											1.2	1.17672
											1.4	1.13713

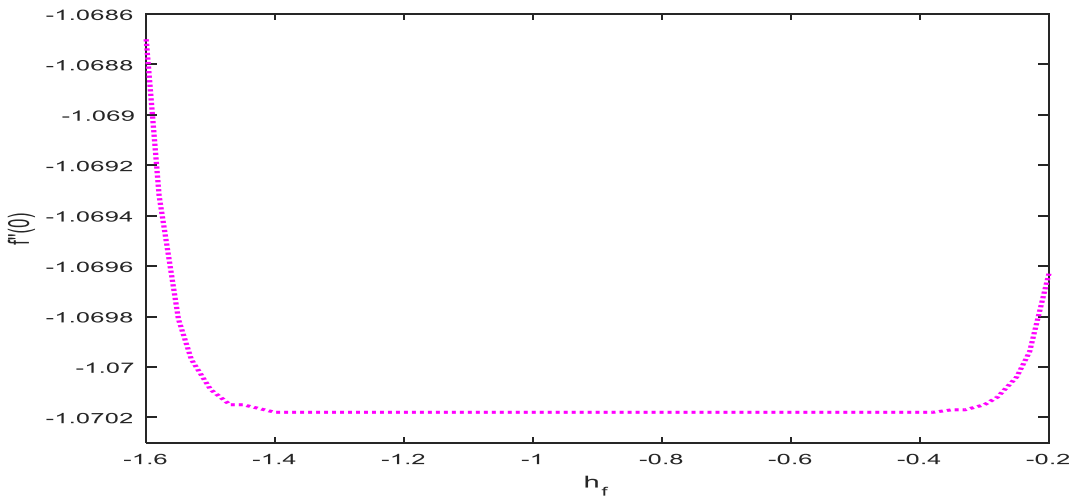

Figure 2: h_f curve

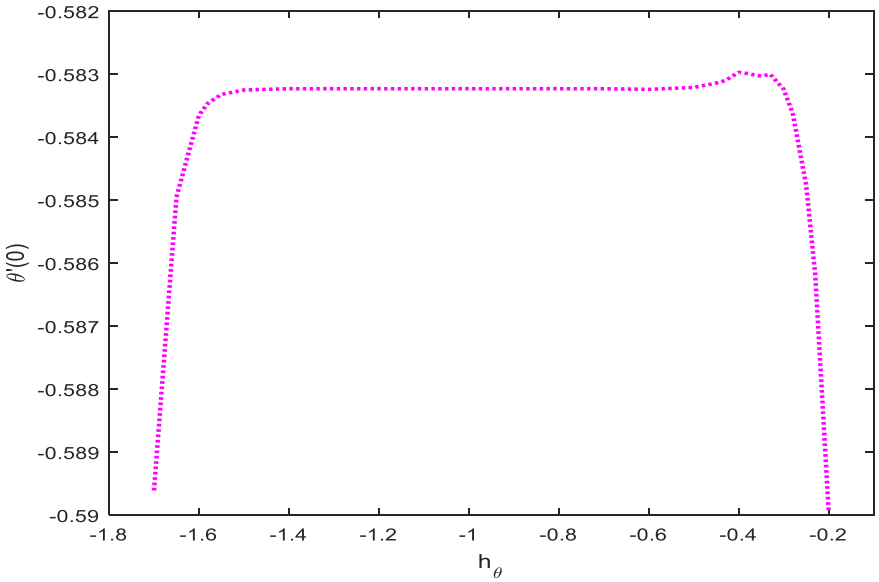

Figure 3: h_θ curve

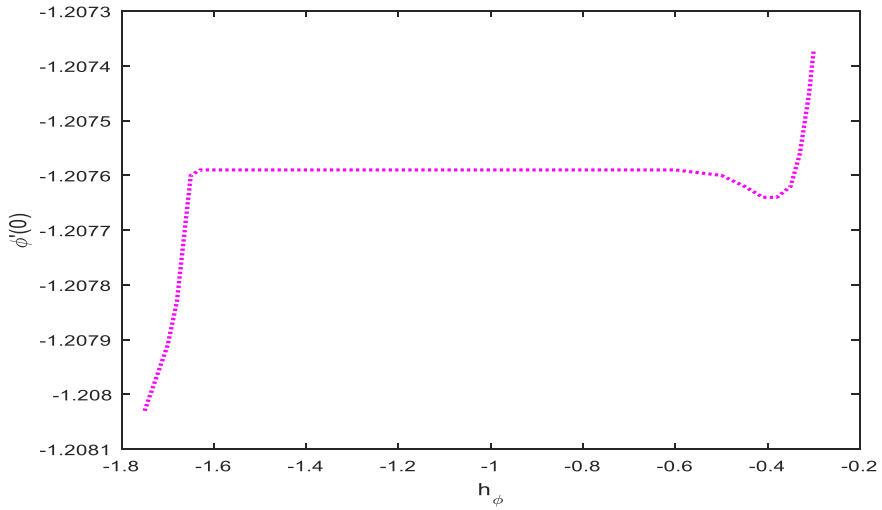

Figure 4: h_ϕ curve

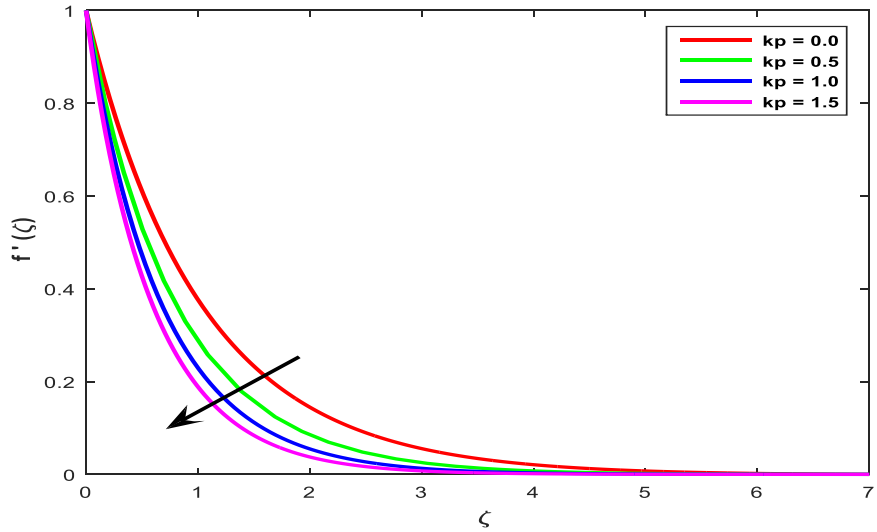

Figure 5:velocity vs. *kp*

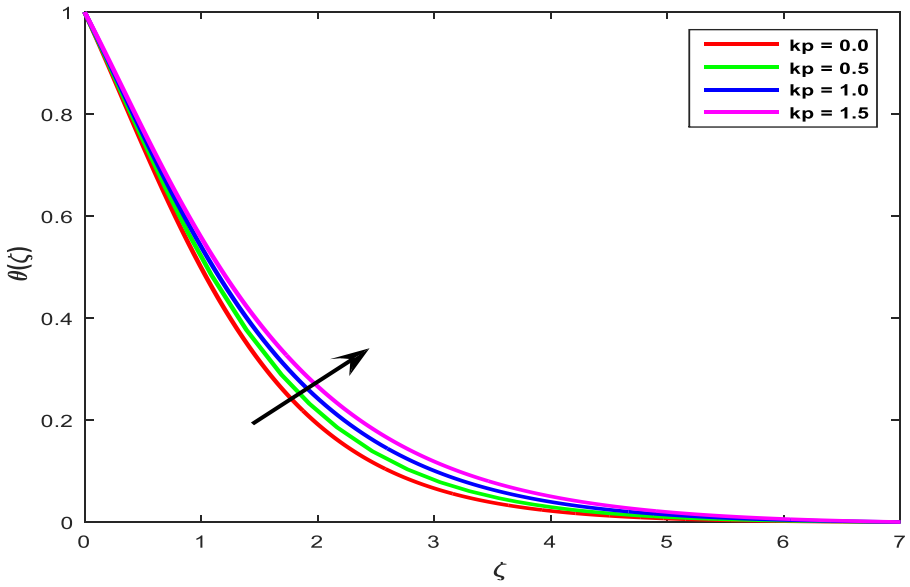

Figure 6: temperature vs. *kp*

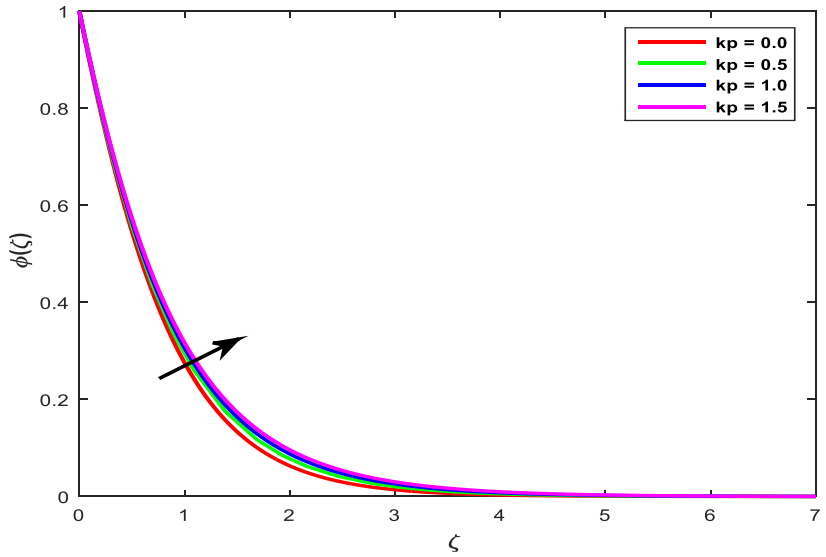

Figure 7: Concentration vs. *kp*

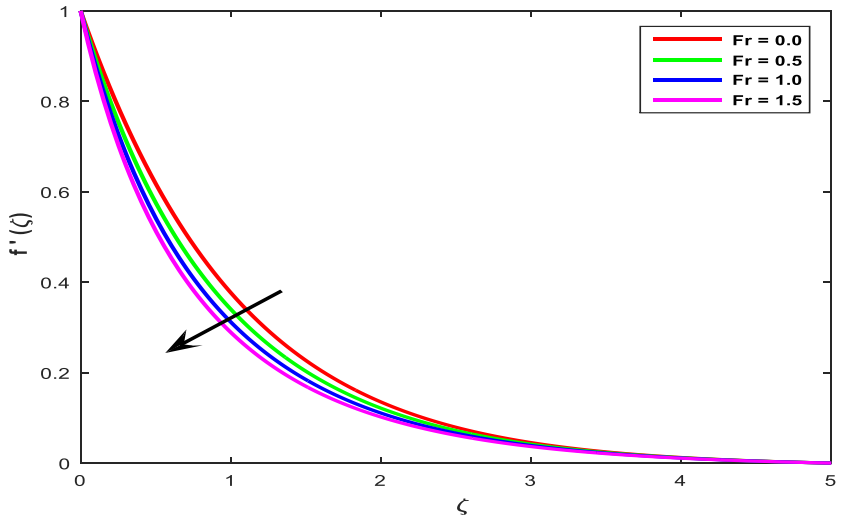

Figure 8: velocity vs. *Fr*

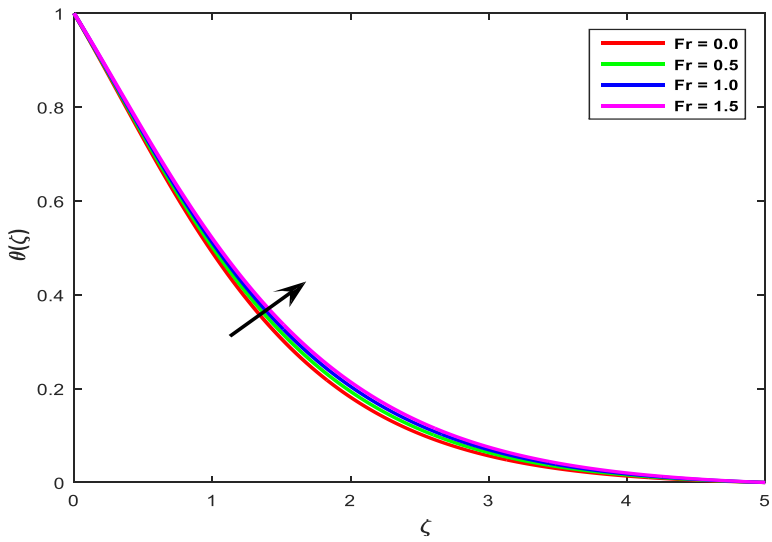

Figure 9: temperature vs. Fr

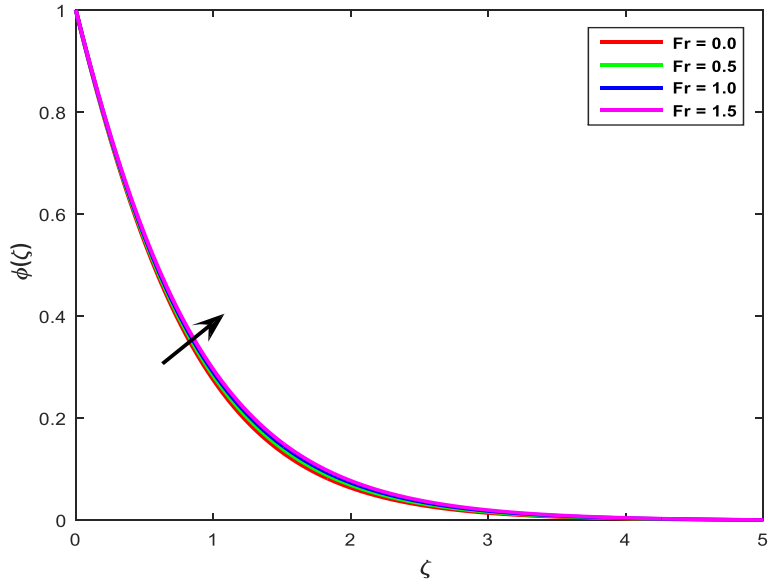

Figure 10: concentration vs. Fr

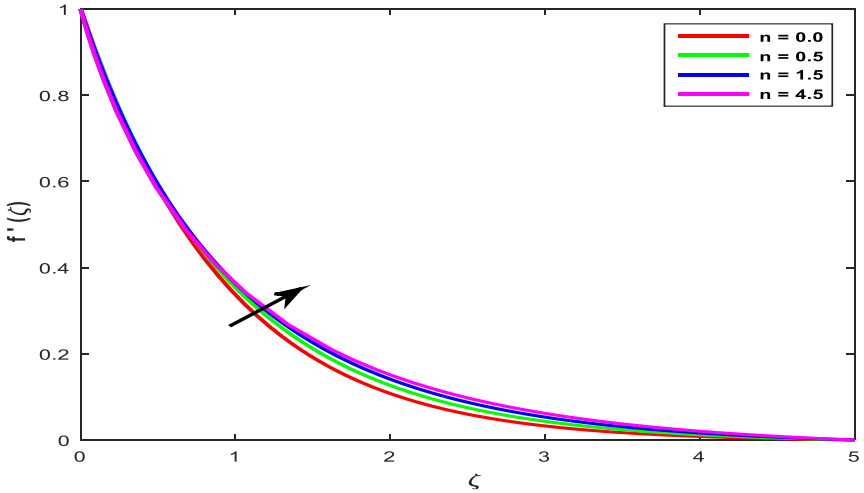

Figure 11: velocity vs. n

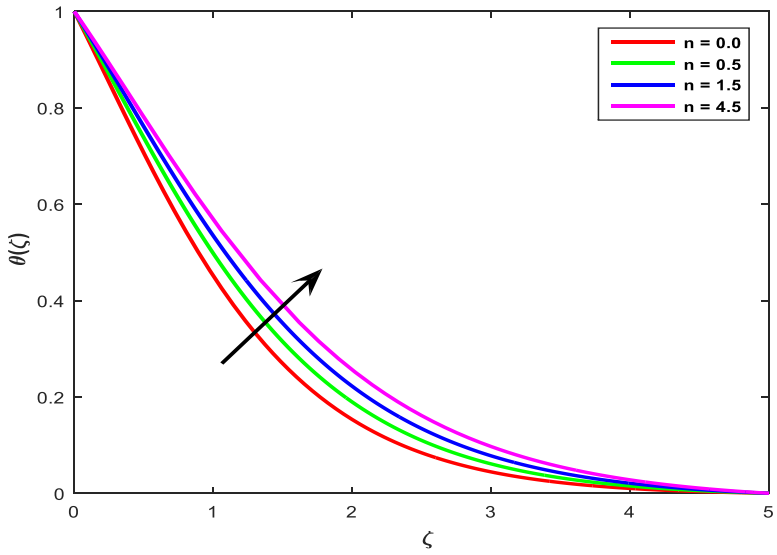

Figure 12: temperature vs. n

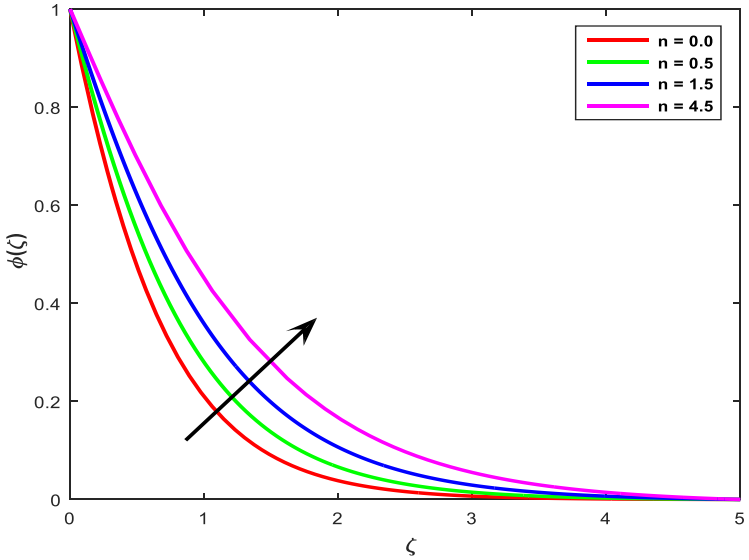

Figure 13: concentration vs. n

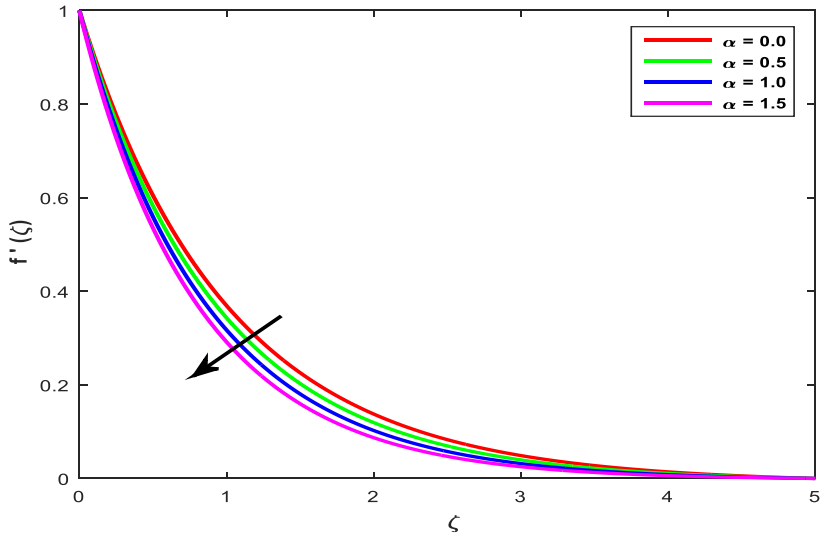

Figure 14: velocity vs. α

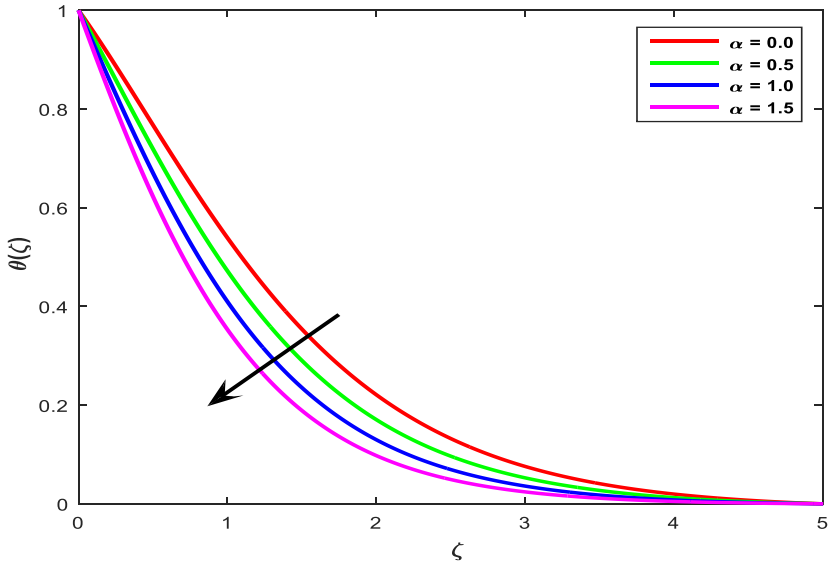

Figure 15: temperature vs. α

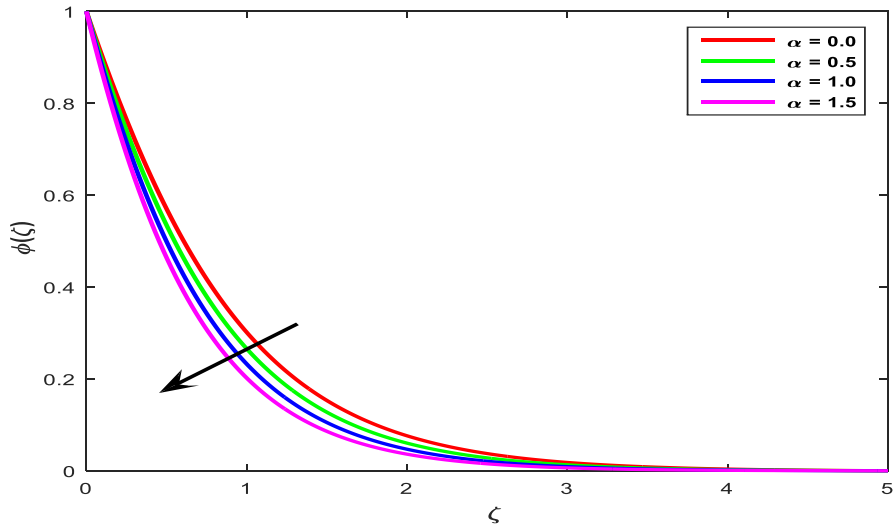

Figure 16: concentration vs. α

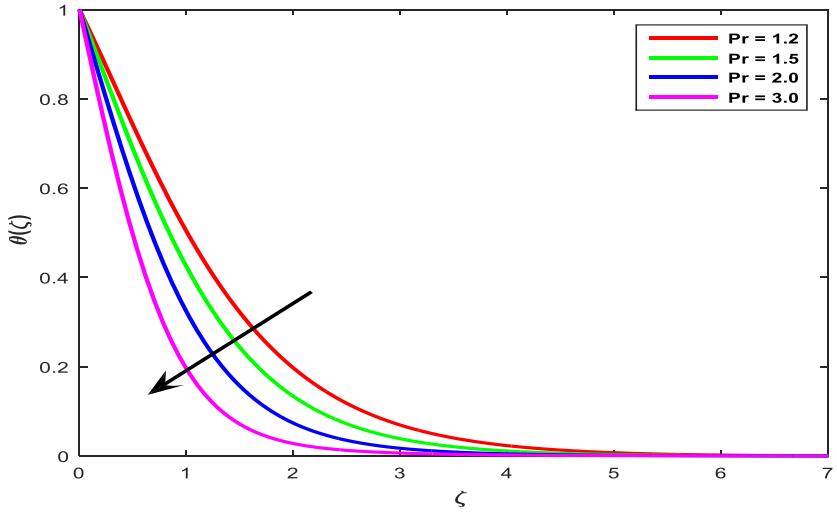

Figure 17: temperature vs. Pr

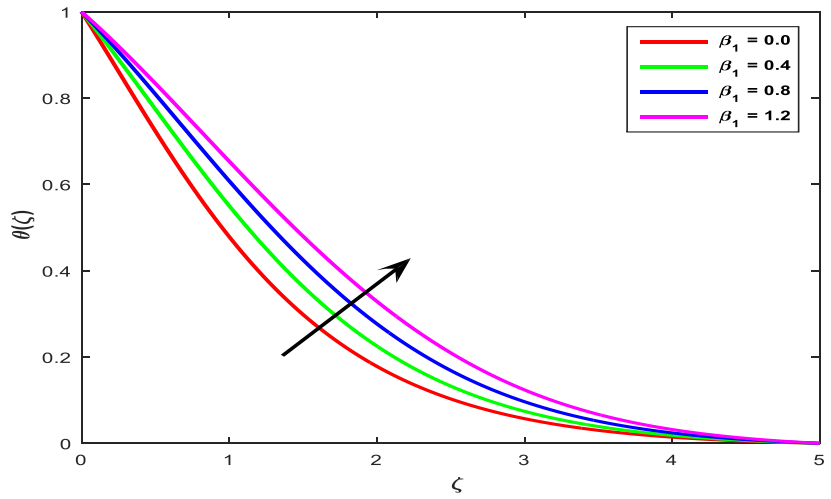

Figure 18: temperature vs. β_1

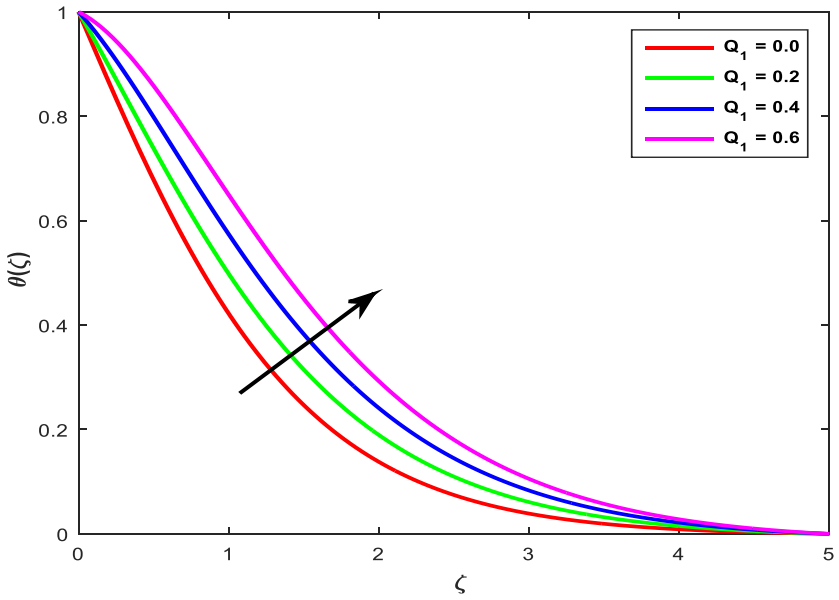

Figure 19: temperature vs. Q_1

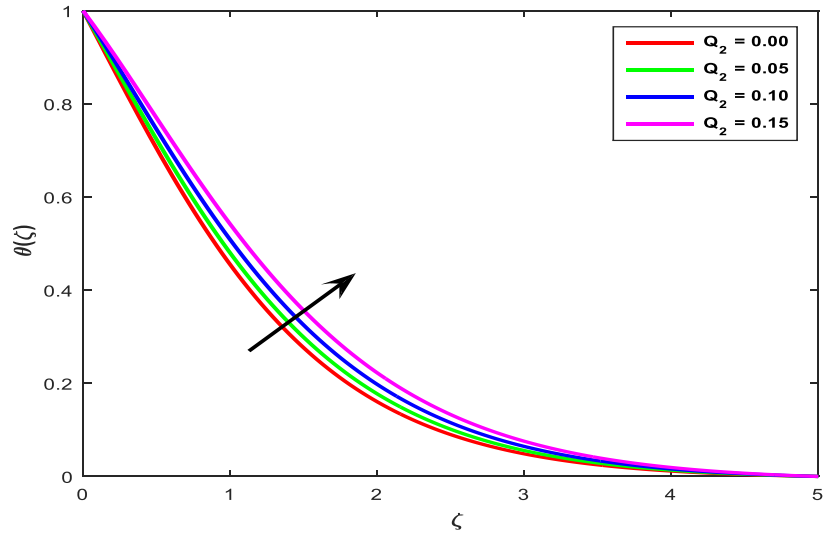

Figure 20: temperature vs. Q_2

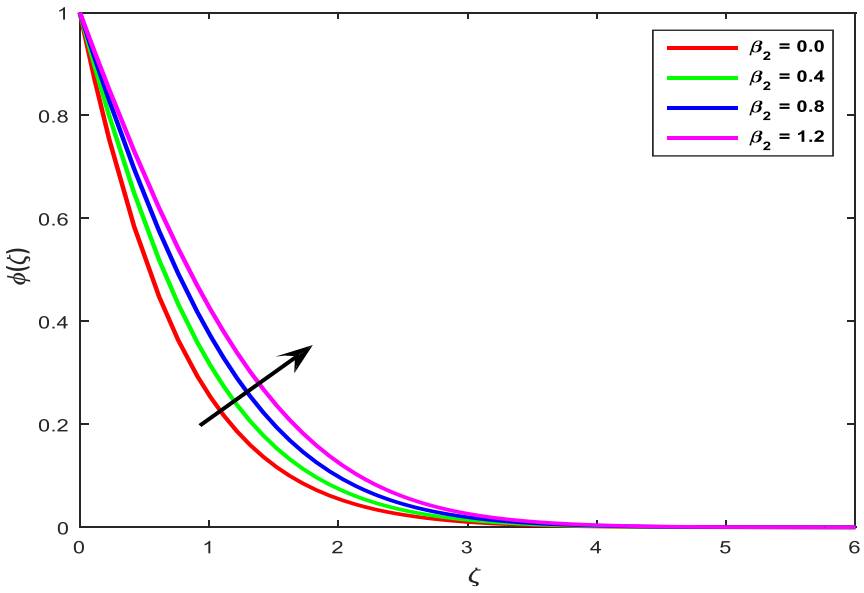

Figure 21: concentration vs. β_2

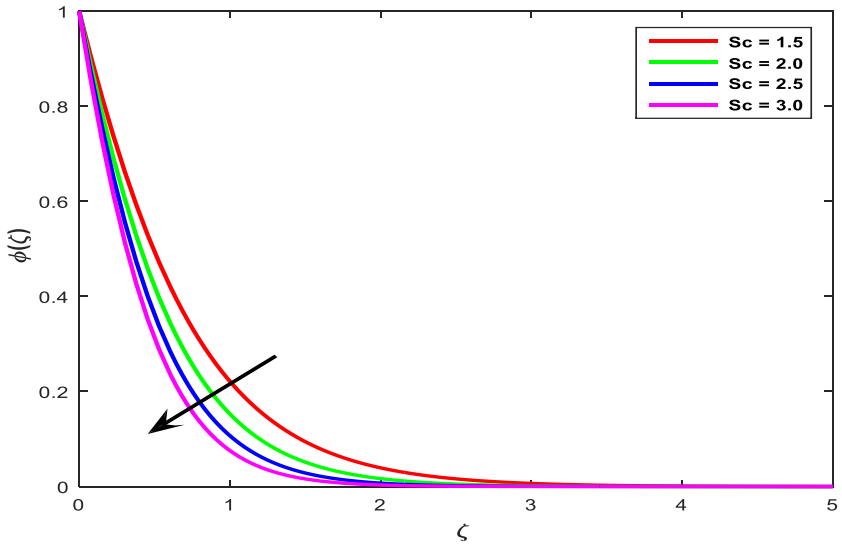

Figure 22: Concentration vs. Sc

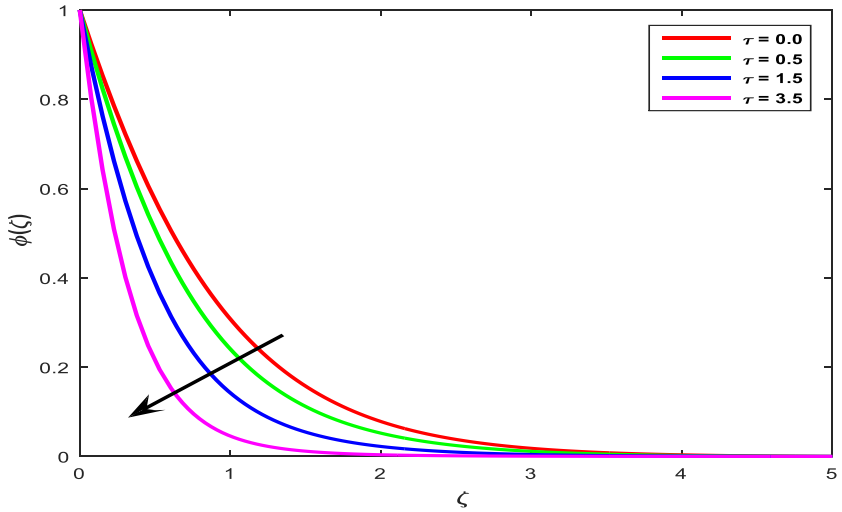

Figure 23: Concentration vs. τ

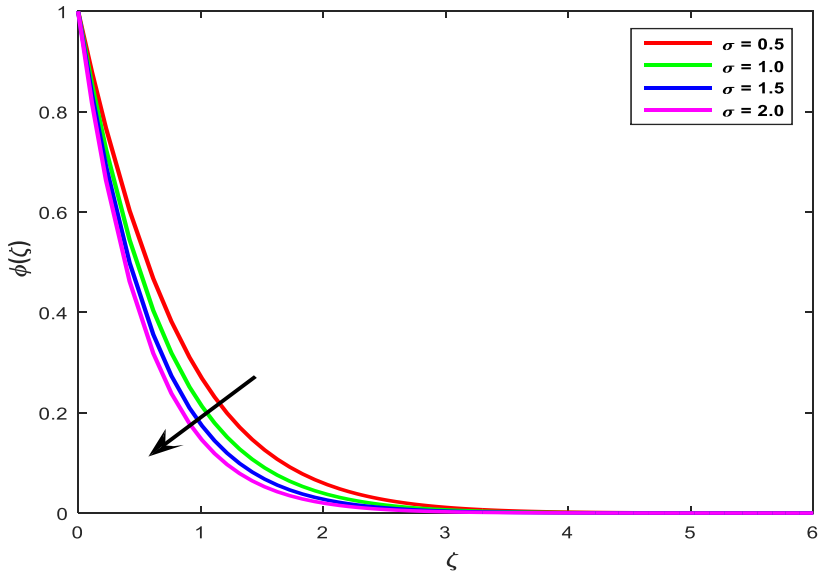

Figure 24: Concentration vs. σ

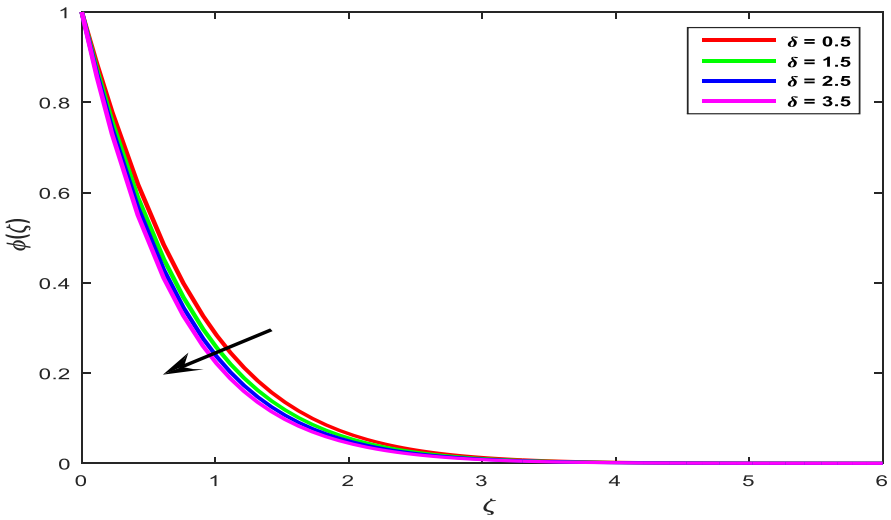

Figure 25: Concentration vs. δ

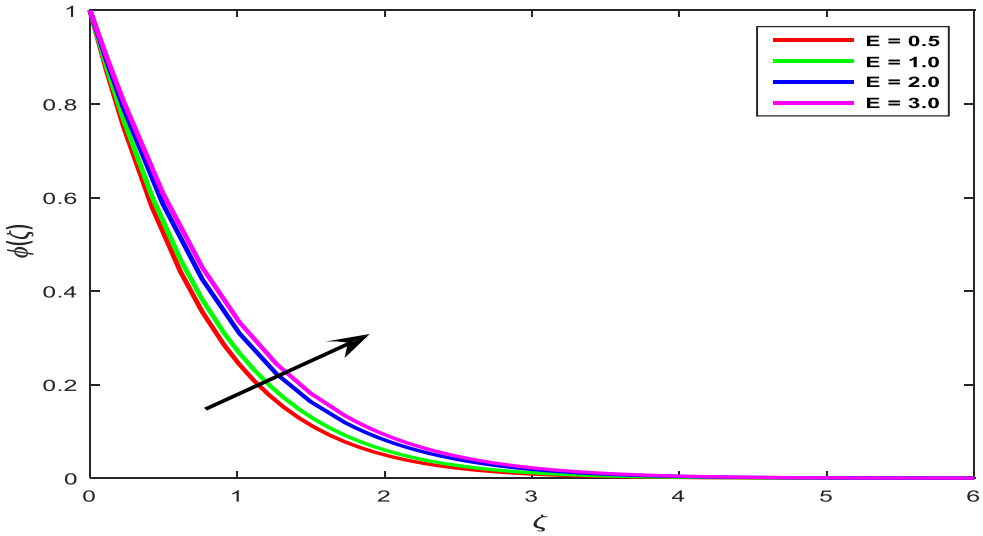

Figure 26: Concentration vs. E

References

1. Hayat, T., Khan, M.I., Waqas, M. andAlsaedi, A., (2017). On Cattaneo-Christovheat flux in the flow of variable thermal conductivity Eyring–Powell fluid. Results Phys; 7:446–50.
2. 2.Jalil, M., Asghar, S. and Imran, S.M.,(2013).Self-similar solutions for theflow and heat transfer of Powell-Eyring fluid over a movingsurface in a parallel free stream. Int.J.Heat Mass Transf; 65:73–9.
3. Akbar, N.S., Ebaid, A. and Khan, Z.H., (2015).Numerical analysis of Magnetic field effect on Eyring-Powell fluid flow towards a stretchingsheet. J.Magn.Mater; 382:355–8.
4. Hayat, T., Awais, M. and Asghar, S., (2013).Radiative effects in a three dimensional flow of MHD Eyring-Powell fluid. J.Egypt.Math.Soc; 21:379–84.
5. 5.Rehman, A., Achakzai, S., Nadeem, S. and Iqbal, S., (2016).Stagnation point flow of Eyring Powell fluid in a vertical cylinder with heattransfer. Journal of Power Technologies; 96:57–62.
6. 6.Qayyum, S., Hayat, T., Shehzad, S.A andAlsaedi, A., (2017).Nonlinear convective flow of Powell-Eyring magneto nano fluid with Newtonian heating. Res.Phys; 7:2933-40.
7. Khan, I., Rehman, K.U. and Malik, M.Y., (2017).Physical aspects of nanoparticles in non-Newtonian liquid in the presence ofchemically reactive species through parabolic approach. Res.Phys; 7:2540–9.
8. Fang, T., Zhang, Ji. And Zhang, Y., (2012).Boundary layer flow over a stretchingsheet with variable thickness. Appl.Math. Comput. 218:7241–52.Doi: 10.1016/j.amc.2011.12.094
9. Khader, M.M., Megahed, A.M., (2013). Numerical solution for boundary layer flow due To a non-linearly stretching sheet with variable thickness and slip velocity.Eur. Phys.J.Plus. 128:100. Doi: 10.1140/ epjp/i2013-13100-7.
10. Abdel-Wahed, M.S., Elbashbeshy, E.M.A. andEmam, T.G., (2015). Flow and heat transfer over a moving surface with nonlinear velocity and variable thickness in a nano fluid in the presence of Brownian motion. Appl. Math. Comput; 254:49–62.
11. Hayat, T., Farooq, M., Alsaedi, A. and Al-Solamy, F., (2015).Impact of Cattaneo–Christov heat flux in the flow over a stretching sheet with variable thickness. AIP Adv.; 5:087159.
12. Hayat, T., Ullah, I., Alsaedi, A. and Farooq, M., (2017).MHD flow of Powell-Eyring nano fluid over a non-linear stretching sheet with variable thickness. Results in Physics,7 189–196.
13. 13.Patil, P. M., Roy, S.,Moitsheki, R. J. and Momoniat, E., (2017).Double Diffusive Flows over a Stretching Sheet of VariableThickness with or without Surface Mass Transfer.Heat Transfer-Asian Research
14. Sudipta, G. and Swathi, M., (2020). MHD mixed convection flow of a nano fluid past a stretching surface of variable thickness and vanishing nano particle flux Pramana.J.Phys. 94:61, 1-12.
15. Sharma, R.P.,Acharya, N. and Das, K.,(2020).On the impact of variable thickness and melting transfer of heat on Magnet to hydrodynamicsnanofluid flow past a slendering stretching sheet. Indian Journal of Geo Marine Sciences Vol. 49 (04), April, pp. 641-648.
16. Irfan, M., Farooq, M.A. and Tousif, I., (2020). A New Computational Technique Design for EMHD Nano fluid Flow over a Variable Thickness Surfacewith Variable Liquid Characteristics Frontier in Physics. Doi: 10.3389/fphy.2020.00066.
17. Qasim, M., Riaz, N., Lu, D. and Afridi, M.I., (2020).Mixed convection flow over a stretching sheet of variable thickness: Analytical andnumerical solutions of self - similar equations. Heat Transfer: DOI: 10.1002/htj.21813.
18. Zahra, A., Khan, I., Waleed, M., Khan, A., Khalil, R., Sayed, E and Sherif, M., (2020).Computational analysis of nano-fluid due to a non-linear variable thicked stretching sheet subjected to Joule heating and thermal radiation. J.Mater.Res.Technol; 9(5):11035–11044.
19. Aleem, M.,Asjad, M.I.,Shaheen, A. and Khan, I., (2020).MHD influence on different water based nanofluids (TiO2, Al2O3, CuO) in porous medium with chemical reaction and Newtonian heating. Chaos Solitons Fractals: 109437.
20. Hayat, T., Saif, R.S.,Ellahi, R., Muhammad, T. and Alsaedi, A.,(2018). Simultaneous effects of melting heat and internal heat generation in stagnation point flow of Jeffrey fluid towards a nonlinear stretching surface with variable thickness, Int. J. Therm. Sci. 132: 344e354.
21. Alshomrani, A.S. andUllah, M.Z., (2019). Effects of homogeneous-heterogeneous

reactions and convective condition in Darcy-Forchheimer flow of carbon nano tubes, J. Heat Tran.141:012405.
22. Seth, G.S. and Mandal, P.K., (2018).Hydromagnetic rotating flow of Casson fluid in Darcy-Forchheimer porous medium, MATEC Web of Conferences, EDP Sciences: Les Ulis, France, 192:02059.
23. Rasool, G.,Chamkha, A.J., Muhammad, T.,Shafiq, A. and Khan, I., (2020). Darcy-Forchheimer relation in Casson typeMHD nanofluid flow over non-linear stretchingSurface Propulsion and Power Research; 9(2):159e168.
24. Ramana Reddy, J.V., Sugunamma, V., Sandeep, N. and Anantha Kumar, K., (2016). Influence of non-uniform heat source/sink on MHD nano fluid flow past aslendering stretching sheet with slip effects. Global Journal of Pure and Applied Mathematics;12 (1).
25. 25.Mehmood, K.,Hussain, S. and Sagheer, M., (2016).Mixed convection flow with non-uniform heat source/sinkin a doubly stratified magnetonanofluid. AIP ADVANCES;6: 065126.
26. 26.Charan Kumar G., Jayarami Reddy, K., Ramakrishna, K. and Narendradh Reddy, M., (2018).Non-Uniform Heat Source/Sink and Joule Heating Effects on Chemically Radiative MHD Mixed Convective Flow of Micropolar Fluid Over aStretching Sheet in Porous Medium Defect and Diffusion Forum; Vol. 388, pp 281-302.
27. Swain1, K., Sampada Kumar, P.,Charan Das, G.,(2018).Effects of Non-Uniform Heat Source/Sink and Viscous Dissipation onMHD Boundary Layer Flow of Williamson Nanofluid through PorousMedium.Defect and Diffusion Forum; Vol. 389, pp 110-127.
28. Anantha Kumar, K.,Ramadevi, B., Sugunamma, V. andRamana Reddy, J. V., (2019).
29. Heat transfer characteristics on MHD Powell-Eyring fluid flow across a shrinkingwedge with non-uniform heat source/sink. Journal of Mechanical Engineering and Sciences.13 (1), pp. 4558-4574. 29. Tyndall, J., (1870).On dust and disease. Proc. R. Inst. G.B. 6, 1–14.
30. Shehzad, S.A., Alsaedi, A. and Hayat, T., (2013).Influence of thermophoresis and joule heating on the radiative flow of Jeffrey fluid with mixed convection.Braz. J. Chem. Eng. 30(4), 897–908.
31. Kameswaran, P.K., Sibanda, P., Partha, M.K. and Murthy, P.V.S.N., (2014). Thermophoretic and Nonlinear Convection in Non-Darcy Porous Medium. ASME J.Heat. Transf. 136: 042601–19.
32. HariprasadRaju, S., Mallikarjuna, B. and Varma, S.V.K., (2015).Effectof Thermophoresison Mixed Convectionflow of a rotating fluid over a rotating cone .Int. J.Sci. Eng. Res. 6(1), 198–204.
33. Mallikarjuna, B., Rashidi, M.M. and Hariprasad Raju, S., (2017).Influence of non-linear convection and thermophoresis on heat and mass transfer from a rotating cone to fluid flow in porous medium.Therm. Sci.Vol. 21, No. 6B, pp. 2781-2793.
34. Bestman, A.R., (1990).Natural convection boundary layer with suction and mass transfer in a porous medium.Int. J. Energy.Res.14 (4):389–96.
35. Makinde, O.D., Olanrewaju, P.O. and Charles, W.M., (2011).Unsteady convection with chemical reaction and radiative heat transfer past a flat porous plate moving through a binary mixture.J.Afrika. Matematika; 22(1):65.
36. Maleque, K.A., (2013).Effects of Binary Chemical Reaction and Activation Energy on MHD Boundary Layer Heat and Mass Transfer Flow with Viscous Dissipation and Heat Generation/Absorption. J. Hindawi. Publ.Corp. Doi: https://doi.org/10.1155/ 2013/284637. Article ID 284637.
37. Awad, F.G., Motsa, S. and Khumalo, M., (2014). Heat and Mass Transfer in Unsteady Rotating Fluid Flow with Binary Chemical Reaction and Activation Energy. J.PLOS.one; Doi: https://doi.org/10.1371/ journal.pone. 0107622
38. Lu, D.C., Ramzan, M., Bilal, M. Chung, J.D. and Farooq U. (2018).A Numerical Investigation of 3D MHD Rotating Flow with Binary Chemical Reaction, Activation Energy and Non-Fourier Heat Flux. J.Commun.Theoret.Phys.70 (1):89–96.
39. Dhlamini, M., Kameswaran, P.K., Sibanda, P., Motsa, S. and Mondal H., (2018). Activation energy and binary chemical reaction effects in mixed convective nanofluid flow with convective boundary conditions. J.Comput. Design. Eng. doi: https://doi.org/10.1016/j.jcde.2018.07.002.
40. Quereshi, I. H., Nawaz, M., Rana, S. and Zubair, T., (2018).Galerkin Finite Element Study on the Effects of Variable Thermal Conductivity and Variable Mass Diffusion Conductance on Heat and Mass Transfer.Commun.Theor.Phys.70, 49– 59.
41. Nawaza, M., Rafiq,S., Qureshi, I.H. and Saleem, S., (2019).Combined effects of

partial slip and variable diffusion coefficient on mass and heat transfer subjected to chemical reaction.Phys. Scr. in press https://doi.org/10.1088/1402-4896/ab534b.

42. Salahuddin, T., Arshad, M., Siddique, N., Alqahatni, A.S. and Malik, M.Y., (2020). Thermophyical properties and internal energy change in Casson fluid flow along with activation energy.Ain.Shams.Engg. Jou., Article in Press.
43. Salahuddin, T., Siddique, N., Arshad, M. and Tlili, I., (2020). Internal energy change and activation energy effects on CassonfluidAIP Advances10 (025009): Doi: 10.1063/1.5140349.
44. Waqas, M., Ijaz Khan, M., Asghar, Z., Kadry, S., Yu-Ming, C., and Khan, W.A. (2020).Interaction of heat generation in nonlinear mixed/forced convective flow of Williamson fluid flow subject to generalized Fourier's and Fick's concept. J.Materres.Technol.9(x x):11080–11086.
45. Waqas, M., Khan, W.A. andAsghar, Z., (2020). An improved double diffusion analysis of non-Newtonian chemicallyreactive fluid in frames of variables properties. International Communications in Heat and Mass Transfer; 115 (2020): 104524.
46. Sajid, T., Sagheer, M. and Hussian, S., (2020).Impact of Temperature-Dependent Heat Source/Sink andVariable Species Diffusivity on Radiative Reiner–Philippoff FluidMath.Prob.Engg. Article ID 9701860. https://doi.org/10.1155/2020/9701860.
47. Irfan, M., Farooq, M.A and Iqra, T., (2020).A New Computational TechniqueDesign for EMHD Nanofluid Flow over a Variable Thickness Surface with Variable Liquid Characteristics.Frontiers in physics; doi: 10.3389/fphy.2020.00066.
48. 48. Liao, S.J., 2012,Homotopy Analysis Method in Nonlinear Differential Equations, Heidelberg: Springer and Higher Education Press.